

ANALYTICAL APPROACH FOR DETERMINATION OF THE BEARING CAPACITY OF RIGID-INCLUSION-IMPROVED FOUNDATIONS

Yuxiang Shen¹, Jesús Pérez-Herreros², Fahd Cui³,
Jean-François Semblat⁴, and Sébastien Burlon⁵

¹ Design engineer, Terrasol (Setec group), Paris, France (yuxiang.shen@setec.com)

² Chief Scientific Officer, Terrasol (Setec group), Paris, France (jesus.perez@setec.com)

³ Chief Executive Officer, Terrasol (Setec group), Paris, France (fahd.cui@setec.com)

⁴ Professor, IMSIA (UMR 9219), CNRS, EDF, ENSTA Paris, Institut Polytechnique de Paris, France (jean-francois.semblat@ensta.fr)

⁵ Former Chief Technical Officer, Terrasol (Setec group), Paris, France (sebastien.burlon@setec.com)

ABSTRACT

The foundations of Nuclear Power Plants (NPP) must meet stringent performance requirements under high gravity loads and seismic conditions. However, natural geotechnical conditions are not always optimal, necessitating ground improvement solutions to enhance bearing capacity and control settlements. One effective technique involves the use of rigid inclusions (RI), which reinforce the soil beneath shallow foundations while incorporating a load transfer platform (LTP) to improve load distribution. Under seismic loading, the LTP may act as a fuse, protecting both the structure and the reinforced soil.

Despite its widespread application in complex geotechnical and seismic contexts, such as the Rio-Antirio bridge and the ICEDA project, the design and verification of foundations on RI-reinforced soil remain insufficiently standardized. This study proposes a novel analytical verification method based on the kinematic approach within the yield design theory framework. The method considers multiple failure mechanisms at both the global scale of the foundation and the local scale of individual inclusions. Fully analytical and easy to implement, this new verification approach aligns with existing methodologies for the verification of bearing capacity of shallow foundations, such as Eurocode EN 1998-5 (CEN, 2007), and can be used directly in both force-based and displacement-based design analyses.

INTRODUCTION

The foundations of Nuclear Powers Plants (NPP), characterised by high loads and stringent performance requirements, need optimum geotechnical conditions. However, these conditions are not always available due to various constraints, such as weak or compressible soils, high seismic hazard and other technical or economic reasons that impose the choice of the location. In such cases, the existing ground may be incapable of supporting the imposed loads or to effectively limit both absolute and differential settlements. To overcome these challenges, ground improvements may be conducted to enhance the ground's bearing capacity and control settlements, ensuring that the site meets the required performance criteria under static and seismic loading conditions.

One possible solution is offered by the ground improvement technique with RI, which presents significant technical and economic advantages. This technique involves a shallow foundation lying on a reinforced soil with vertical rigid elements, known as inclusions, which are physically disconnected from the structures they support. Instead, a load transfer platform (LTP) is incorporated between the head of the inclusions and

the structure, as illustrated in Figure 1. Furthermore, under high-intensity seismic loading, the LTP can act as a fuse, protecting both the supported structure and the reinforced soil.

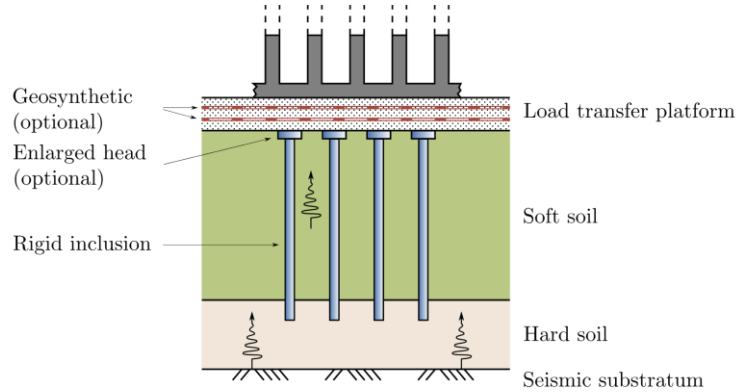


Figure 1. Shallow foundation reinforced soil by rigid inclusions under seismic loading

This solution has been successfully implemented in numerous projects presenting complex geotechnical and seismic contexts, such as the Rio-Antirio bridge (Pecker and Teyssandier, 2009) and the ICEDA project (Mattsson et al., 2013). It has gained important attention from the industry and has motivated several research projects and guidelines over the last two decades, such as ASIRI French National project (ASIRI, 2012). However, several aspects regarding the design and verification of this type of foundation under complex loads have not yet been properly addressed nor standardized. This gap has motivated recent research works within the ASIRI+ French National research project (Briançon et al., 2021).

Assessing the bearing capacity of the foundation under static and seismic loadings is essential for the correct design and verification of the structure. Standardized approaches are already available and used today to address this question in the case of shallow and deep foundations. They are in most cases derived from numerical or analytical approaches, such as the yield design theory (Salençon, 1983) which has proven its effectiveness and accuracy in predicting the ultimate bearing capacity of shallow foundations, providing a rigorous and scientifically grounded approach, such as Eurocode EN 1998-5 (CEN, 2007).

The study presented in this article addresses the issue of determining the bearing capacity of shallow foundations on improved soil with rigid inclusions via a new analytical approach formulated using the kinematic exterior approach within the framework of yield design theory. This method incorporates a multi-criterion strategy to deal with the various failure mechanisms likely to be mobilised in this type of foundation, both at the global scale of the reinforced soil-foundation system and at the local scale corresponding to the stability of each one of its reinforcements (e.g. structural resistance, interaction with the soil, etc.).

ÉTAT DE L'ART

Theoretical framework: kinematic exterior approach

Within the framework of the yield design theory (Salençon, 1983), the kinematic exterior approach functions as an upper-bound analysis method. This approach involves defining a kinematically admissible virtual velocity field $\underline{\hat{U}}$ and ensuring that the virtual power of external loads applied to the system, denoted as P_e , does not exceed the maximum resisting power of the soil, denoted as P_{rm} . An upper-bound K encompasses the space delineated by following equation:

$$K \subset \{P_{rm}(\underline{\hat{U}}) \geq P_e(\underline{\hat{U}})\} \quad (1)$$

The maximum resisting power P_{rm} is equal to:

$$P_{rm}(\underline{U}) = \int_{\Omega} \pi(\hat{\underline{d}}) d\Omega + \int_{\Sigma} \pi([\underline{\hat{U}}]) d\Sigma \quad (2)$$

where $\pi(\cdot)$ represents the density of virtual power due to the strain rate $\hat{\underline{d}}$ within the volume Ω and to the virtual velocity $[\underline{\hat{U}}]$ at the velocity discontinuity surface Σ . These quantities are computed from the strength criteria. The explicit formulation of the function $\pi(\cdot)$ for various criteria, applicable to both continuous materials and interfaces, can be found in the work of Salençon (1983).

The virtual power of all external forces P_e applied to the system includes the contribution of the seismic loads acting on the foundation as well as the body forces resulting from soil inertia, representing the seismic acceleration in the soil. For a foundation reinforced with RI, the formulation of P_e remains identical to that of an unreinforced foundation. Additionally, the presence of RI introduces a contribution to the resisting power, denoted by P_{RI} , which should be incorporated, as outlined in the following equation.

$$K \subset \{P_{rm}(\underline{U}) + P_{RI}(\underline{U}) \geq P_e(\underline{U})\} \quad (3)$$

Application to the analysis of geotechnical structures

The kinematic exterior approach has been extensively applied to solve shallow foundation bearing capacity problems. Previous studies have used this method to evaluate the bearing capacity of strip foundations on homogeneous cohesive and cohesionless soils under both static and seismic loading conditions (Salençon and Pecker, 1995a, 1995b; Paolucci and Pecker, 1997).

In the work of Salençon and Pecker (1995b), a tension cut-off condition to the soil strength criterion is introduced, allowing to describe a purely cohesive medium with no tensile strength. The investigated failure mechanisms investigated are depicted in Figure 2. The rotation-translation kinematically admissible failure mechanisms \underline{U} , both without and with uplift, are illustrated in Figure 2 (a) and (b), respectively. Additionally, several mechanisms involving only a rigid block in rotation were also proposed, as shown in Figure 2 (c) and (d).

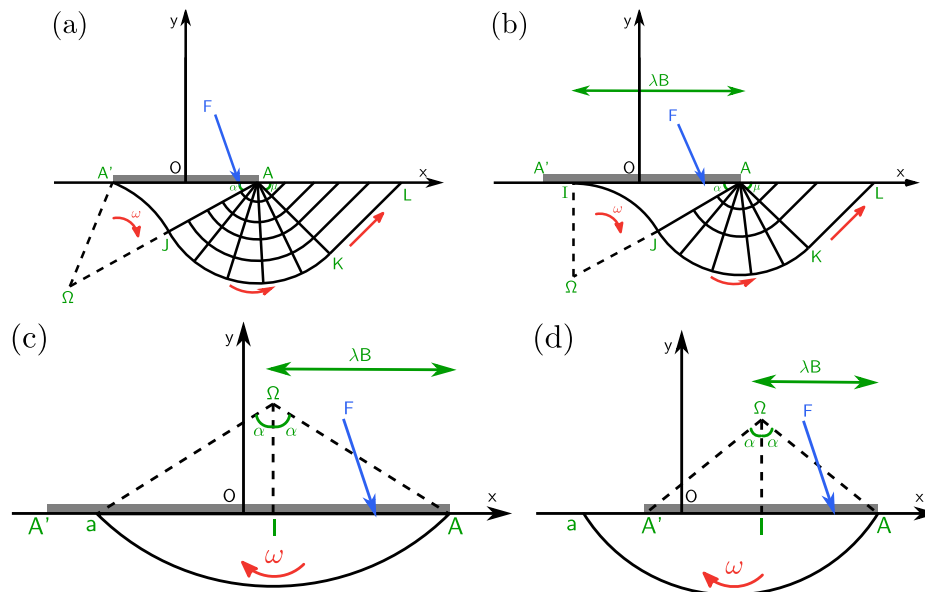


Figure 2. Velocity fields for a rigid strip foundation on coherent (unreinforced) soil

The kinematic exterior approach has also been applied to analyze the stability of reinforced geotechnical structures, such as nailed slopes. de Buhan et al. (1992) investigated the stability of nailed slopes using this approach, considering kinematic mechanisms based on triangular blocks and logarithmic spiral failure surfaces. Notably, several slope stability software programs, such as Talren (Terrasol, 2023), incorporate failure surfaces in the form of logarithmic spirals. The contribution of nail reinforcements is introduced by employing a multicriterion approach based on various failure modes associated with the nails.

However, the application of the kinematic exterior approach to the study RI-reinforced foundations remains limited. This is largely due to the inherent complexity introduced by the coexistence of the three distinct components in such reinforced foundation system: the soft soil, the granular LTP, and the RI. This complexity makes it challenging to define the kinematically admissible virtual velocity fields \hat{U} used in the kinematic exterior approach.

Pecker et al. (1998) were the first to determine the seismic bearing capacity of a shallow foundation on cohesive soil reinforced by RI, in a remarkable use of the kinematic exterior approach. The retained virtual velocity field is illustrated in Figure 3. The contribution of the RI to the overall stability was considered by the intrinsic material resistance and their skin friction. Additionally, a failure criterion representing the slide failure between the LTP was introduced as well. The results of this analytical model were compared with five centrifuge tests conducted for the Rio-Antirrio bridge project, showing a good performance in predicting the bearing capacity of this foundation configuration.

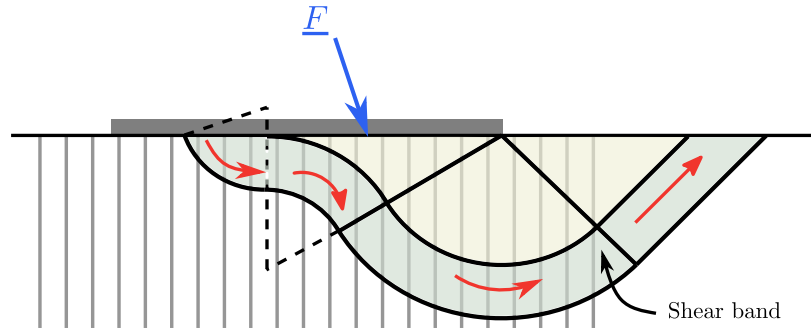


Figure 3. Virtual velocity field considered in the bearing capacity assessment of the Rio-Antirrio bridge foundation adapted from Pecker et al. (1998)

BEARING CAPACITY OF RIGID-INCLUSION-IMPROVED FOUNDATION

Statement of the problem: A strip foundation improved by rigid inclusions

This section investigates the seismic bearing capacity of a strip foundation on a reinforced soil by with RI. The foundation, of width B , rests on a three-layer half-space consisting of a LTP of thickness h_{LTP} , exhibiting purely frictional behavior, characterized by a friction angle φ . Beneath the LTP lies a cohesive soft soil layer with cohesion c and non tensile strength. The layer is reinforced with RI, as illustrated in Figure 4. Finally, a seismic substratum is found at the base of the soft soil layer.

The RI-improvement is modelled by means of embedded beams that are regularly spaced by a distance s beneath the foundation and extend down to the underlying substratum. The (inclined) load transmitted to the foundation is denoted as F and can also be expressed by its horizontal and vertical component, noted H and V respectively. The moment M is calculated as the product of the vertical force and the eccentricity e . Furthermore, soil inertia effects are accounted for through body forces induced by seismic and gravitational loading, expressed as $f_x = \rho a_x$ and $f_y = \rho(g \pm a_y)$, respectively.

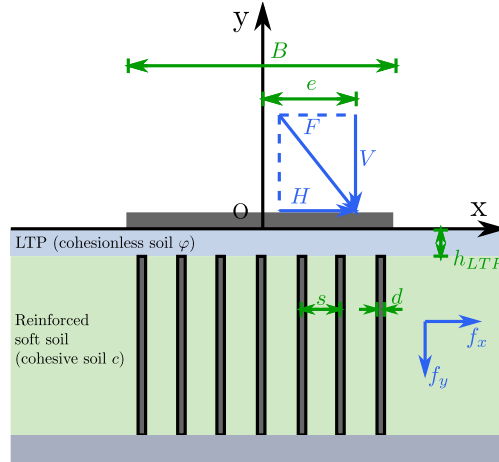


Figure 4. Studied configuration: strip foundation on reinforced soil by RI

Potential failure mode

The presence of the reinforcements and the LTP layer introduces additional complexity to the failure mechanisms when compared to unreinforced soil configurations. To address this question, three simplified sub-systems, illustrated in Figure 5, are studied separately, each one corresponding to a different “family” of potential failure mechanisms:

- Case I: This sub-system considers a homogeneous frictional soil, where the failure mechanism is primarily confined within the LTP, leading to a failure depth shallower than h_{LTP} .
- Case II: This sub-system accounts for potential sliding and uplift at the interface between the LTP and the reinforced soft soil.
- Case III: This sub-system represents a homogeneous cohesive soil reinforced with RI where the failure mechanism extends beyond h_{LTP} , intersecting the RI-improvement, which consequently contributes to the overall resistance. The contributions of both the soil and the RI are evaluated separately, as illustrated in Figure 6.

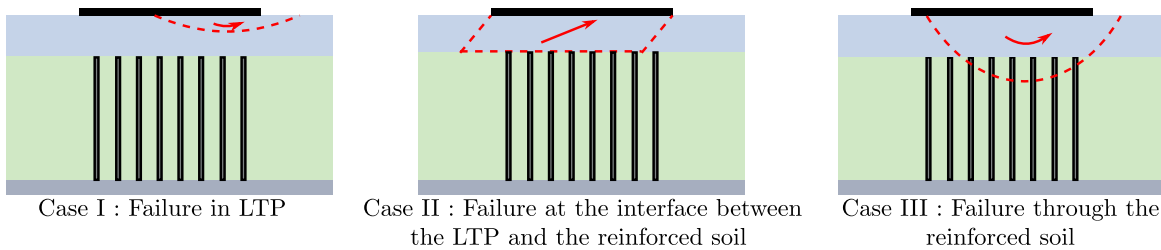


Figure 5. Simplified sub-systems accounting for different types of potential failure mechanisms

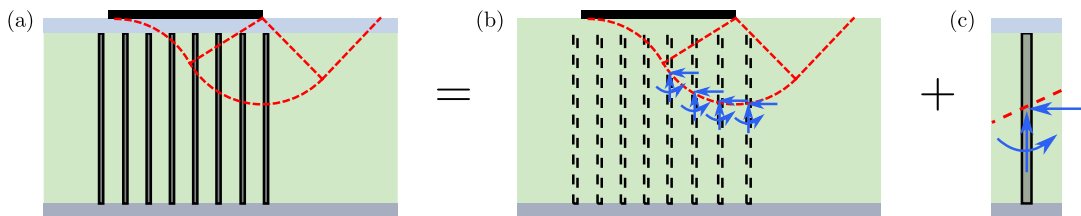


Figure 6. Detailed description of Case III sub-systems: (a) multi-block failure mechanism, (b) simplified configuration, and (c) forces at the intersection of RI with the surface of the failure mechanism

The upper-bound solutions for the three cases are denoted $K^{up,I}$, $K^{up,II}$, and $K^{up,III}$. They are combined to determine the stability domain K^{up} of a foundation reinforced by RIs, as described in following equation:

$$K^{up} = K^{up,I} \cap K^{up,II} \cap K^{up,III} \quad (4)$$

Failure analysis of a rigid inclusion

The RI are considered by accounting for their action at the intersection with the failure surface. The RI is divided into two parts by the intersection: interior part with a length L_{int} and exterior part with length L_{ext} . The forces at this intersection are decomposed into an axial force T_n , a shear force T_c , and a bending moment M_c . The force combination (T_n, T_c, M_c) should be limited by the different kinds of potential failure modes of RI.

- Material intrinsic strength

The combination of T_n , T_c , and M_c need to respect the following inequality to ensure that the strength of the material is not exceeded. R_n , R_c , and R_m are the limits of the material intrinsic strength for axial force, shear force, and bending moment respectively. The corresponding criterion is represented by the curve (1) in Figure 7.

$$\left(\frac{T_n}{R_n}\right)^2 + \left(\frac{T_c}{R_c}\right)^2 + \left|\frac{M_c}{R_m}\right| - 1 \leq 0 \quad (5)$$

- Axial soil-inclusion interaction resistance

The maximum axial force T_{nl} that a RI of diameter d can provide is also governed by parameters such as the skin friction, the forces at the head and the tip of the RI, and the internal “pullout” failure mechanism. This can be described by equation (6).

$$T_n \leq T_{nl} = \min(F_0 + q_s L_{int} \pi d, F_L + q_s L_{ext} \pi d) \quad (6)$$

where F_0 represents the maximum force controlled by a Prandtl failure mechanism that develops in the LTP, F_L represents the maximum force at the inclusion tip, which is typically of significant magnitude, and q_s denotes the characteristic value of the inclusion shaft friction. This axial soil-interaction failure corresponds to the line (2) in Figure 7.

- Lateral soil-inclusion interaction resistance

This criterion represents the mobilized resistance resulting from lateral soil-inclusion interaction, which is analyzed using a limit equilibrium model. Various assumptions regarding the distribution of soil pressure on the RI are examined. Further details can be found in Shen (2023). Two possible scenarios are considered: In the first one, the soil pressure acting on the RI reaches its limiting value p_l^* , leading to a failure of the surrounding soil. In the second, the applied pressure generates a significant bending moment in the RI before reaching the limiting pressure. These two scenarios are represented by interaction curves (3) and (4) in Figure 7, respectively.

The combination of the four criteria in the T_n - T_c plane defines a stability domain, referred to as the RI multicriterion, as illustrated in Figure 7. At failure, the resisting forces developed by the RI must lie on the boundary of this domain, with their exact position governed by the principle of maximum work. According to this principle, the resisting forces are distributed in a manner that maximizes the contribution of the RI to the overall resistance within a given failure mechanism. Once the virtual velocity at the intersection

between the inclusions and the failure surface is defined, the corresponding virtual power $P_{RI}(\underline{U})$ of the inclusions can be computed.

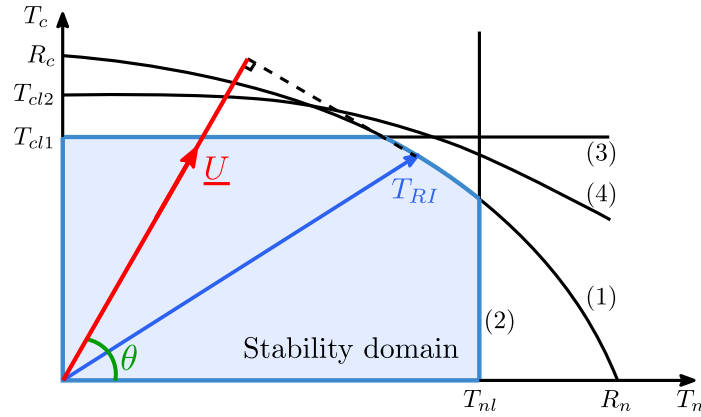


Figure 7. Multicriterion in the $T_n - T_c$ plane representing the resistance of a RI

Numerical applications

The foundation configuration illustrated in Figure 4 is considered in this numerical application. The system consists of a strip footing of width $B = 10$ m, resting on a LTP with a thickness of 0.5 m and a friction angle φ of 38° . The soft soil is considered cohesive with no tensile strength, exhibiting an undrained cohesion c of 25 kPa. Based on this cohesion, the ultimate lateral friction q_s and the limit pressure p_l^* are estimated at 25 kPa and 200 kPa, respectively. The unit bearing resistance of the soil beneath the inclusion tip, q_b , is set to 2 MPa. The RI-improvement, arranged in seven rows, has a diameter d of 0.4 m and a length L of 10 m. They are installed beneath the foundation, with no embedment into the LTP layer, and are spaced of $s = 1.5$ m. The substitution ratio α for this configuration is 5.6 %.

The interaction diagrams for this configuration, derived from the study of the three types of failure modes (see Figure 5), are presented in Figure 8 (a). These three interaction curves delineate an admissible zone, referred to as the potential stability domain, as illustrated in Figure 8 (b). It is important to note that the ultimate bearing capacity under a vertically centered load for a foundation on RI-reinforced soil is governed by failure mode III, in which the failure mechanism extends through the reinforced soil mass, engaging the rigid inclusions in the resistance mechanism.

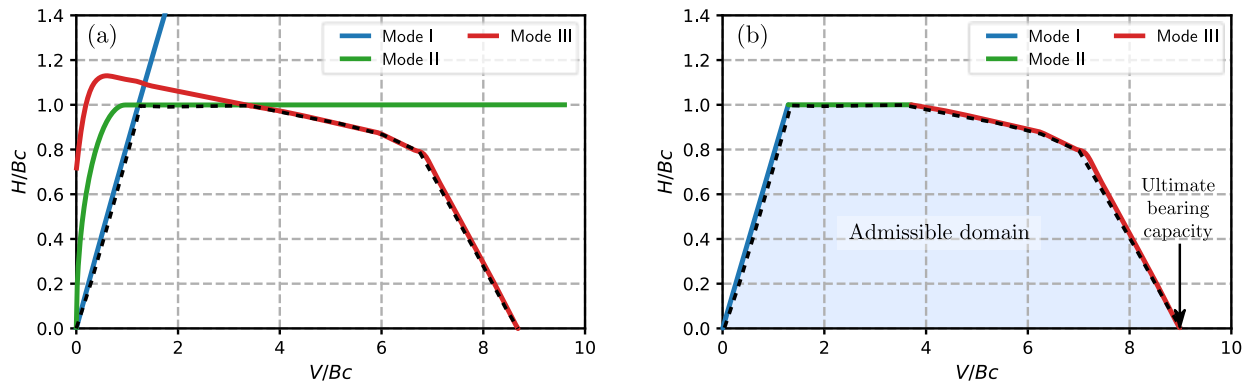


Figure 8. (a) Interaction diagrams from the three failure modes and (b) stability domain of a foundation on reinforced soil with RI in the standard $V - H$ plane.

REDUCTION FACTOR IN THE BEARING CAPACITY FORMULATION

Having established an analytical approach to determine the bearing capacity of a given foundation on a reinforced soil with RI, it is possible to investigate how the bearing capacity is influenced by load eccentricity, load inclination and soil inertia effects. In conventional force-based design, the verification framework involves comparing the applied vertical load V with its limit value V_{max} , according to the criterion:

$$V - V_{max} \leq 0 \quad (7)$$

To account for seismic effects, the limit value V_{max} may be modified by applying specific reduction factors, leading to the revised verification criterion:

$$V - V_{max} i_e i_\delta i_g \leq 0 \quad (8)$$

where i_e represents the load eccentricity reduction factor, i_δ is the load inclination reduction factor, and i_g accounts for the soil inertia reduction factor. The evolution of these three reduction factors depending on different parameters is studied in the following section.

Studied configurations

A 10-meter-wide strip foundation, reinforced with seven rows of inclusions, as shown in Figure 4, is considered in the following numerical applications. Three different diameters of the inclusions, 0.2 m, 0.4 m, and 0.55 m, are used, corresponding to substitution ratios α of 1.4%, 5.6%, and 10.6%, respectively. In addition, an unreinforced configuration that incorporates a frictional LTP layer is also studied for comparison.

Load eccentricity effect

The effect of load eccentricity is first investigated by varying the eccentricity of a vertical load applied on the foundation. Figure 9 (a) presents the bearing capacities for different configurations and eccentricities, including the case without rigid inclusions. A consistent trend is observed across all cases: as the load eccentricity increases, the ultimate bearing capacity decreases. Among the reinforced configurations, a higher substitution ratio consistently results in a greater bearing capacity.

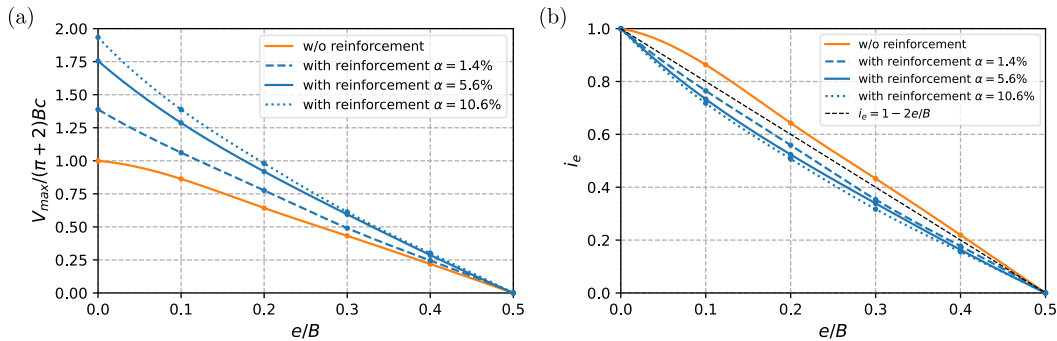


Figure 9. Evolution of (a) bearing capacity, and (b) eccentricity reduction factor i_e with load eccentricity

The reduction ratio, defined as $i_e = V_{max,e}/V_{max,e=0}$, is illustrated in Figure 9 (b) and compared with the analytical expression $i_e = 1 - 2e/B$ for the unreinforced configuration. The results indicate that load eccentricity has a more pronounced effect on rigid inclusion-reinforced foundations than on unreinforced

ones. In other words, they are more sensitive to load eccentricity. For instance, at an eccentricity ratio of $e/B = 0.2$, the strip foundation retains 64% of its ultimate bearing capacity, whereas the RI-reinforced foundation with a substitution ratio of 5.6% retains only 53%.

Load inclination effect

The bearing capacity of a non-reinforced strip foundation is reduced when subjected to combined inclined loading effects. An evaluation of the bearing capacity under inclined loading for various studied configurations is presented in Figure 10 (a). The results are shown as a function of the load inclination δ , normalized by the friction angle φ of the LTP. The effect of reinforcement on bearing capacity is particularly evident for load inclination angles smaller than 0.5φ . However, for load inclinations exceeding this threshold, the bearing capacity values for both reinforced and unreinforced configurations become nearly identical, indicating that the benefits of the reinforcement diminish under strongly inclined loads. The inclination reduction factor $i_\delta = V_{max,\delta}/V_{max,\delta=0}$ is presented in Figure 10 (b). It can be observed that the load inclination reduction factor i_δ for the unreinforced foundation is consistently higher than that for the reinforced configurations, suggesting that they are more sensitive to load inclination.

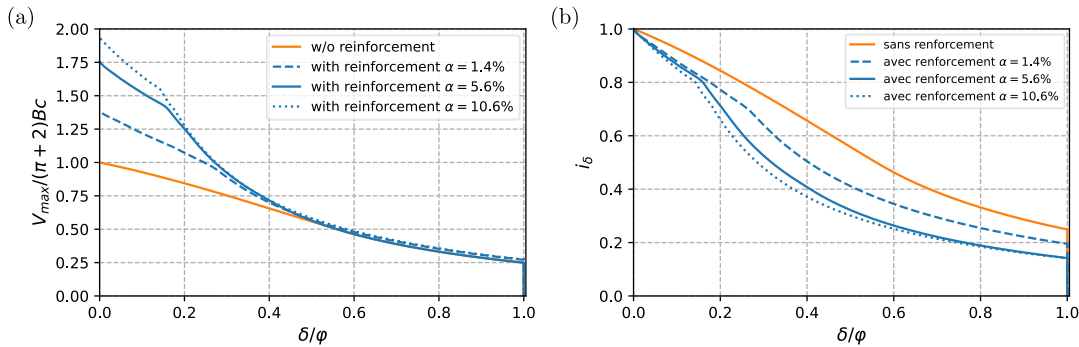


Figure 10. Evolution of (a) bearing capacity, and (b) inclination reduction factor i_δ with load inclination

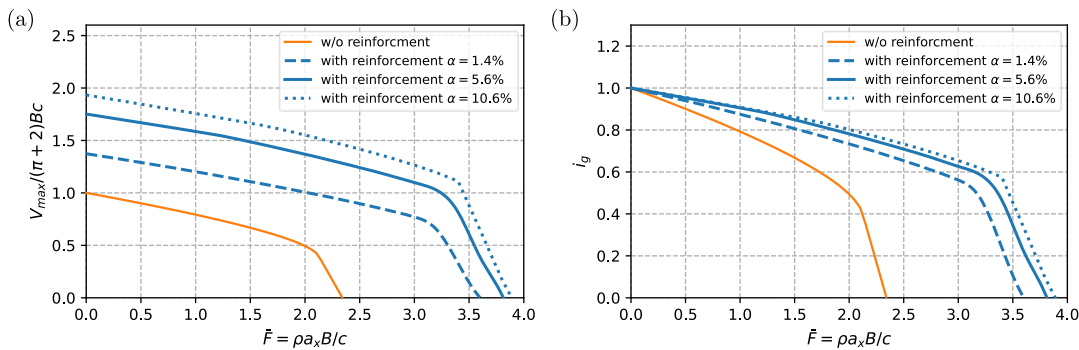


Figure 11. Evolution of (a) bearing capacity, and (b) soil inertia reduction factor i_g with soil inertia

Soil inertia effect

Figure 11 (a) presents the evolution of the bearing capacity for different soil inertia values, represented by the dimensionless soil inertia forces $\bar{F} = \rho a_x B/c$. When comparing the unreinforced configuration to the reinforced ones, it is evident that the reinforcement improves the ultimate bearing capacity under a vertical centered load V_{max} , enabling the foundation to better withstand soil inertia. Figure 11 (b) illustrates the reduction in bearing capacity caused by soil inertia, represented by $i_g = V_{max,a_x}/V_{max,a_x=0}$. This factor decreases as soil inertia increases across all studied configurations. Notably, the bearing capacity of the

reinforced foundations declines at a slower rate as soil inertia intensifies. This observation highlights the reinforcement's ability to enhance the resilience of the foundations under seismic excitation.

CONCLUSION

A novel analytical approach to determine the bearing capacity of foundations on reinforced soil by rigid inclusions has been developed within the framework of yield design theory. This method integrates three failure modes, along with an innovative multi-criterion approach specifically designed for rigid inclusions, to determine the stability domain of the foundation. This method is on the continuity of existing approaches for the static and seismic bearing capacity assessment of shallow foundations, making it directly applicable to the design of foundations with rigid inclusions. It is fully analytical and allows a rapid evaluation of the bearing capacity using a limited number of parameters, thus providing preliminary insights for detailed design. Furthermore, it can be easily implemented in a spreadsheet or script, both for forced-based and displacement-based verification analyses.

The study also investigates reduction factors for load eccentricity and inclination, demonstrating that foundations on soil reinforced by rigid inclusions exhibit greater sensitivity to the effects of load eccentricity and inclination. However, despite the more adverse correction factors, the overall bearing capacity of foundations with rigid inclusions remains, in all cases, superior or equal to that of non-reinforced foundations. Additionally, the investigation into the effects of soil inertia confirms that the use of rigid inclusions significantly mitigates the impact of soil inertia caused by seismic motion. This finding further supports the benefits of using RI-reinforced foundations in areas with high seismic risk.

REFERENCES

- European Committee for Standardization (CEN). (2007). *Eurocode 8: Design of structures for earthquake resistance - Part 5: Foundations, retaining structures and geotechnical aspects*. AFNOR.
- ASIRI (2012). *Recommandations pour la conception, le calcul, l'exécution et le contrôle des ouvrages sur sols améliorés par inclusions rigides verticales*. Presses des Ponts.
- Briançon, L., Simon, B., and Thorel, L. (2020). "Le projet ASIRI+: Amélioration et Renforcement des Sols par Inclusions Rigides,". *Proc., JNGG2020*, Lyon, France.
- de Buhan, P., Dormieux, L., Salençon, J. (1992). "An interactive computer software for the yield design of reinforced soil structures". *Proc. Colloque International Informatique et Géotechnique*, Paris, France.
- Mattsson, N., A. Menoret, C. Simon, and M. Ray (2013). "Case study of a full-scale load test of a piled raft with an interposed layer for a nuclear storage facility," *Geotechnique*, 63(11), 965–976.
- Optum Computational Engineering (2021). *OPTUM G2*. Copenhagen, Denmark.
- Paolucci, R., Pecker, A. (1997). Seismic bearing capacity of shallow strip foundations on dry soils. *Soils and foundations*, 37(3), pp.95-105.
- Pecker, A., Harikiopoulos, H., de Buhan, P., Dormieux, L., Morand, P. (1998). *Comportement sismique d'une fondation sur sol renforcé par inclusions rigides*, Compte rendu pour MRES, Paris, France.
- Salençon, J. (1983). *Calcul à la rupture et analyse limite*, Presses des Ponts.
- Salençon, J., Pecker, A. (1995a). "Ultimate bearing capacity of shallow foundations under inclined and eccentric loads. Part I: purely cohesive soil," *European journal of mechanics series a solids*, 14, pp. 349-349.
- Salençon, J., Pecker, A. (1995b). "Ultimate bearing capacity of shallow foundations under inclined and eccentric loads. Part II: purely cohesive soil without tensile strength," *European journal of mechanics series a solids*, 14, pp. 377–96.
- Shen, Y. (2023). *Development of a macro-element of foundations under dynamic load: Application in the case of soils reinforced by rigid inclusions*. Doctoral dissertation, Institut Polytechnique de Paris.
- Terrasol (2023) *TALREN (v6): Advanced slope stability analysis with or without reinforcements*, Paris, France.